

Supporting Information

A Size-shrinkable Nanoparticle-based Combined Anti-tumor and Anti-inflammatory Strategy for Enhanced Cancer Therapy

Zhengze Lu, Yang Long, Xingli Cun, Xuhui Wang, Jianping Li, Ling Mei, Yiliang Yang, Man Li, Zhirong Zhang and Qin He*

Key Laboratory of Drug Targeting and Drug Delivery Systems, West China School of Pharmacy, Sichuan University, No. 17, Block 3, Southern Renmin Road, Chengdu 610041, China

*Corresponding author: Tel/Fax: +86-28-85502532; E-mail: qinhe@scu.edu.cn

Materials and Animals

Materials.

c(RGDfK)-Cys peptide (sequence c[Arg-Gly-Asp-(D-Phe)-Lys]-Cys) was synthesized by China Peptides Co., Ltd. (Shanghai, China) through standard solid-phase peptide synthesis. NH₂-PEG-COOH (MW 5000) and Maleimide-PEG-Succinimidyl Valerate (MAL-PEG-SVA, MW 3400) were obtained from Seebio Biotech. Co., Ltd. (Shanghai, China). DGL-NH₂ G3 TFA COUNTER-ION (DGL) was purchased from Colcom Co., Ltd. (Montpellier Cedex, France). Gelatin type A was obtained from MP Biomedicals Co., Ltd. (California, USA). Doxorubicin hydrochloride and metformin hydrochloride were obtained from Meilun Biotech Co., Ltd. (Dalian, China). 1-[3-(dimethylamino)propyl]-3-ethylcarbodiimide hydrochloride (EDC), N-Hydroxy-succinimide (NHS) and p-carboxybenzaldehyde (p-CBA) were purchased from J&K Scientific Co., Ltd. (Beijing, China). Glutaraldehyde solution (Grade II, 25% in water) was purchased from Solarbio Technology Co., Ltd. (Beijing, China). Agarose L.M.P (Low gelling temperature) was obtained from Biosharp Co., Ltd. (Hefei, China). Lipopolysaccharides from *Escherichia coli* O55:B5 (LPS) was purchased from Sigma-Aldrich (USA). 3-(4,5-dimethyl-2-thiazolyl)-2,5-diphenyl-2-H-tetrazolium bromide (MTT), 4',6-diamidino-2-phenylindole (DAPI), fluorescent mounting media, LysoTracker Red (DND-99), enhanced BCA protein assay kit, sodium dodecyl sulfate polyacrylamide gel electrophoresis (SDS-PAGE) kit, SDS-PAGE sample loading buffer (5X) and NF- κ B p65 rabbit pAb were purchased from Beyotime Biotechnology (Shanghai, China). GAPDH antibody and goat anti-rabbit IgG (H+L) HRP were purchased from Abways Technology (USA). Cyanine5.5 NHS ester (Cy5.5-NHS) was purchased from Lumiprobe Corporation (Maryland, USA). Nuclear and cytoplasmic protein extraction kit was purchased from KeyGen Biotech. Co., Ltd. (Nanjing, China). Mouse TNF- α ELISA Kit (96T) was purchased from Colorfulgene (Wuhan, China). Amicon Ultra 15 mL centrifugal filters (MWCO 10 kDa) were purchased from Millipore (USA). Dialysis bag (MWCO 3.5 kDa, 10 kDa) was purchased from Spectrumlabs (USA). The other inorganic reagents are all analytically pure.

Cell Lines and Animals.

Mouse breast cancer cells (4T1) and colorectal cancer cells (CT26) were obtained from Shanghai Institutes for Biological Sciences, CAS (SIBS, Shanghai, China). 4T1 cells were cultured in Dulbecco's modified Eagle's medium (DMEM, Hyclone) containing 10% FBS (Gibco), 100 U mL⁻¹ penicillin and 100 μ g mL⁻¹ streptomycin at 37 °C, 5% CO₂ atmosphere in a humidified incubator. CT26 cells were cultured in RPMI 1640 medium (Gibco) containing 10% FBS (Hyclone), 100 U/mL penicillin and 100 μ g/mL streptomycin under the same culture condition. Balb/c mice (about 5-week-old, 18-22g, female, SPF) were purchased from Dashuo Experimental Animal Company (Chengdu, China). The feeding conditions of all mice were consistent. All animal experiments were performed in compliance with the rules of Experimental Animals Administrative Committee of Sichuan University and Chinese National Standard for Laboratory Animals.

Synthesis and Preparation

Preparation of Gelatin Nanoparticles (GNP).

GNP was prepared using a two-step desolvation method as previously described with some improvement.¹ In brief, gelatin type A (500 mg) was dissolved in 10 mL of deionized water in a 25 mL beaker in 40 °C oil bath. The beaker was sealed with plastic film and 12 mL of acetone was added into the beaker at the speed of 6 mL min⁻¹ through a 20 mL injector under the stirring speed of 300 rpm. Then stopped stir immediately and let the solution stand for 1 min, discarded the upper fluid. Residual gelatinous precipitate was dissolved using 10 mL of deionized water in 40 °C oil bath. The pH value of the solution was adjusted to 2.7 using 1 M HCl and the solution was transferred into a 100 mL round bottomed flask. 25 mL of acetone was added into the flask using a needle through the rubber plug under the stirring speed of 600 rpm in 40 °C oil bath. 36 µL of glutaraldehyde solution (Grade II, 25% in water) was diluted in 0.8 mL of acetone and was added in the above reaction system at the speed of 0.03 mL min⁻¹. After the addition of glutaraldehyde, the stirring speed was adjusted to 1,000 rpm and the mixture was stirred for 4 h in 40 °C oil bath. The acetone was removed using a rotary evaporator till the residue volume was about 10 mL. Then 200 µL of glycine aqueous solution (1 M) was added to terminate the cross-linking reaction. The product was stored in refrigerator at 4 °C overnight and was separated by a Sephadex G50 column using pH 6.0 PBS as mobile phase. UV absorption was detected at 254 nm wavelength and the end-product (GNP solution) was collected (1.5 mL product per 1 mL sample).

Preparation of p-Carboxybenzaldehyde-Metformin (pCM) and p-Carboxybenzaldehyde-Doxorubicin (pCD).

To prepare pCM, metformin hydrochloride (300 mg) and p-carboxybenzaldehyde (p-CBA, 350 mg) was dissolved in 25 mL of methanol and the mixture was stirred in 35 °C oil bath overnight. The crude product was condensed to about 2 mL and was purified by column chromatography (solid phase: silica gel GF₂₅₄, mobile phase: dichloromethane-methanol (4 : 1, v/v)). The outflow was sampled using capillary tubes and monitored by thin-layer chromatography (TLC). The collected mixture was vaporized using a rotary evaporator to obtain the pCM product.

To prepare pCD, doxorubicin hydrochloride (DOX·HCl, 350 mg) was dissolved in 5 mL of dimethyl sulfoxide (DMSO) together with 270 µL of triethylamine (triple amount of DOX·HCl). The mixture was stirred overnight to remove the hydrochloric acid. Then p-CBA (300 mg) was dissolved in 8 mL of DMSO and added into the mixture in the previous step. The mixture was stirred at room temperature for 72 h. The crude product was purified by column chromatography (solid phase: neutral alumina, mobile phase: dichloromethane-methanol (1 : 1, v/v)). The outflow was sampled using capillary tubes and monitored by thin-layer chromatography (TLC). The collected mixture was vaporized using a rotary evaporator to obtain the pCD product. The successful preparation of pCM and pCD was confirmed by ¹H-NMR spectrum.

Experimental Procedures

Serum Stability Assay.

The serum stability of RDDG NPs and RMDG NPs was evaluated by both turbidimetric method and dynamic light scattering (DLS) measurement. According to a fixed volume ratio (Sample : FBS (v/v) = 1 : 1 and 9 : 1), samples were mixed with fetal bovine serum (FBS) (final FBS volume ratio was 50% and 10%).

Turbidimetric method: The mixed sample was transferred into a 96-well plate (200 μL per well) and incubated at 37 $^{\circ}\text{C}$, 75 rpm for 48 h. The absorbance of samples was measured under UV detection mode at 750 nm using a Varioskan Flash Multimode Reader (Thermo, USA) at each time point (0, 1, 2, 4, 8, 12, 24 and 48 h).

DLS measurement: The mixed sample was incubated under 37 $^{\circ}\text{C}$, 75 rpm for 48 h. The variation of particle size was measured by Malvern Zetasizer Nano ZS90 (Malvern, U.K.) at each time point (0, 1, 2, 4, 8, 12, 24 and 48 h).

In Vitro Hemolysis Assay.

A hemolysis assay was performed to evaluate the safety of RDG NPs. The mass of RDG NPs in per milliliter solution was determined by freeze-drying. About 0.8 mL of whole blood was collected from mice orbit and centrifuged at 1500 rpm for 5 min. The supernatant was discarded and remains (mainly red blood cells) were washed with pH 7.4 PBS for 3 times, and prepared 2% RBC (red blood cell) suspension (20 μL RBC/1 mL PBS). The RDG NPs solution was mixed with equal volume of 2% RBC suspension respectively. The final material concentrations were 3.0, 1.5 and 0.75 mg mL^{-1} , respectively ($n = 4$). PBS suspension was used as negative control group and 0.5% Triton X-100 suspension was used as positive control group. All groups were incubated in shaking bed at 37 $^{\circ}\text{C}$, 75 rpm for 8 h. A small amount of supernatant was taken after 1500 rpm, 5 min centrifugation as test samples at different time points (1, 2, 4, 8h), and test samples were added into a 96-well plate (100 μL /well) and the absorption was measured at 540 nm using a Varioskan Flash Multimode Reader (Thermo, USA).

$$\text{Hemolysis Ratio (\%)} = (A_{\text{Sample}} - A_{\text{PBS}}) / (A_{\text{Triton X-100}} - A_{\text{PBS}}) \times 100\%$$

Supplementary Tables

Table S1. The screening of synthetic conditions of GNP (Means \pm SD, n = 3). Data in the last line were the synthetic conditions used.

Gelatin Type A (mg)	Oil bath (°C)	DW* for the 1 st time dissolving (mL)	DW* for the 2 nd time dissolving (mL)	25% Glutaraldehyde solution (μ L)	Cross-linking time (h)	PDI	Size (nm)
500	45	12.5	6	48	7.5	0.164 \pm 0.011	403.2 \pm 66.3
500	45	12.5	10	48	7.5	0.216 \pm 0.015	264.9 \pm 18.8
500	45	10	10	48	7.5	0.207 \pm 0.005	223.6 \pm 21.4
500	40	10	10	48	7.5	0.178 \pm 0.013	172.0 \pm 12.5
500	40	10	10	36	7.5	0.139 \pm 0.020	118.1 \pm 1.0
500	40	10	10	36	4	0.092 \pm 0.009	98.6 \pm 5.7

*DW = Deionized Water

Table S2. Characterization of different NPs (Means \pm SD, n = 3).

	PDI	Size (nm)	Zeta Potential (mV)	Drug Loading Capacity (%)
RD NPs	0.153 \pm 0.017	28.48 \pm 2.56	-0.37 \pm 0.18	N/A
RDG NPs	0.203 \pm 0.015	113.8 \pm 3.6	-6.11 \pm 0.53	N/A
RDDG NPs	0.207 \pm 0.026	133.3 \pm 3.7	-7.05 \pm 0.62	6.72 \pm 1.01 (DOX)
RMDG NPs	0.168 \pm 0.014	124.4 \pm 3.4	-5.74 \pm 0.25	3.96 \pm 0.84 (MET)

Supplementary Figures

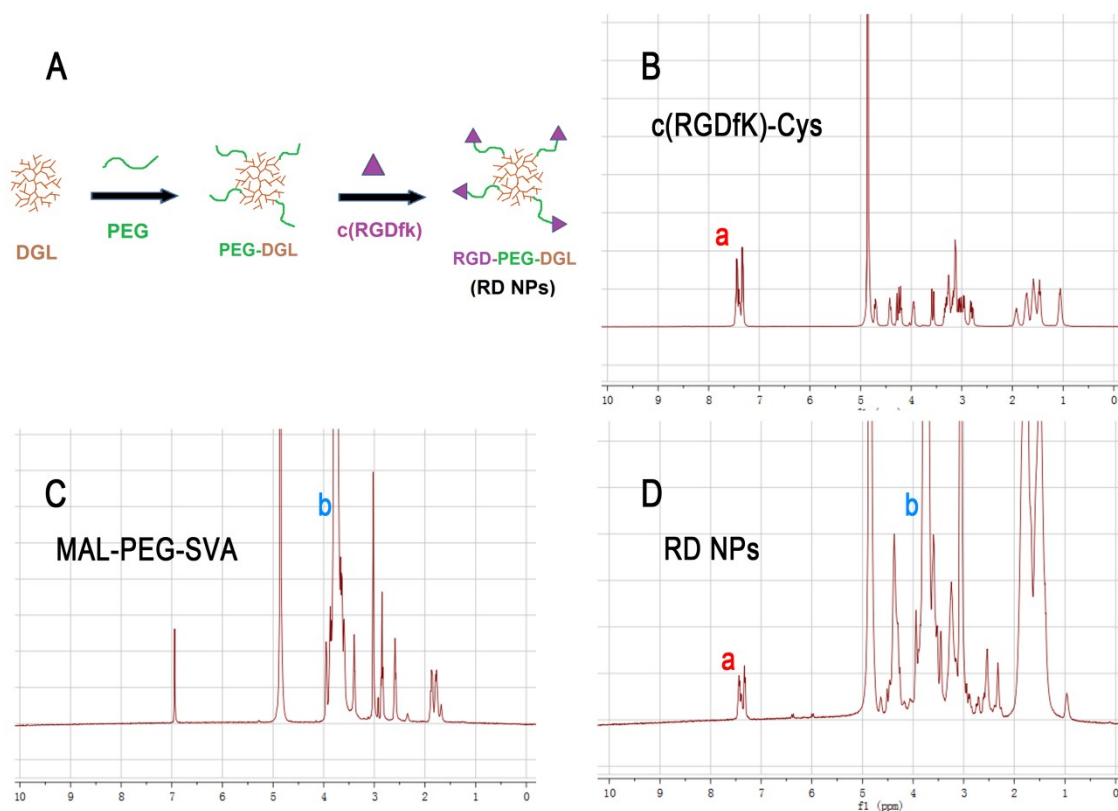


Figure S1. (A). Schematic illustration of RGD-PEG-DGL (RD NPs). The ¹H-NMR spectrum of (B) c(RGDfk)-Cys, (C) MAL-PEG-SVA and (D) RD NPs (in D₂O). a. Characteristic peak of the aromatic group in c(RGDfk)-Cys. b. Characteristic peak of PEG chain. These two peaks indicated the successful synthesis of RD NPs.

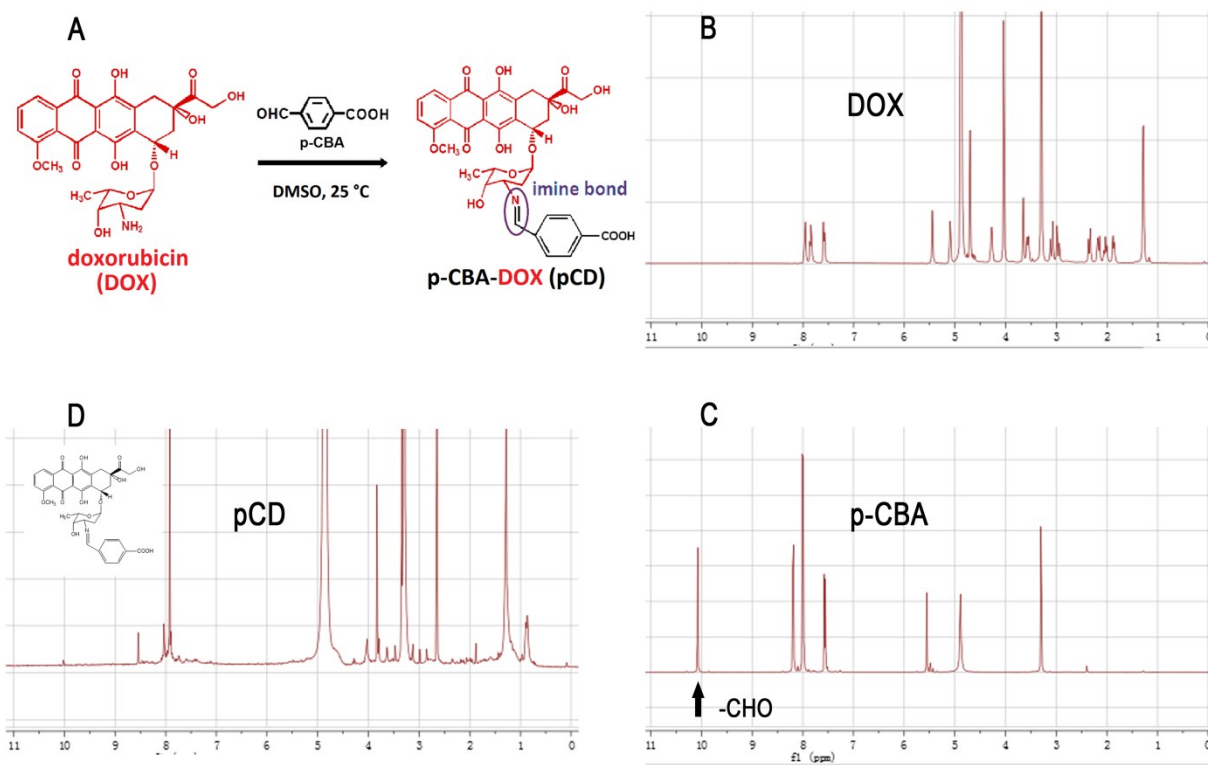


Figure S2. (A). Schematic illustration of p-CBA-DOX (pCD). The $^1\text{H-NMR}$ spectrum of (B) DOX, (C) p-CBA and (D) pCD (in CD_3OD). The arrow in (C) indicated the characteristic peak of aldehyde group in p-CBA. This peak disappeared in (D), indicating the formation of imine bonds.

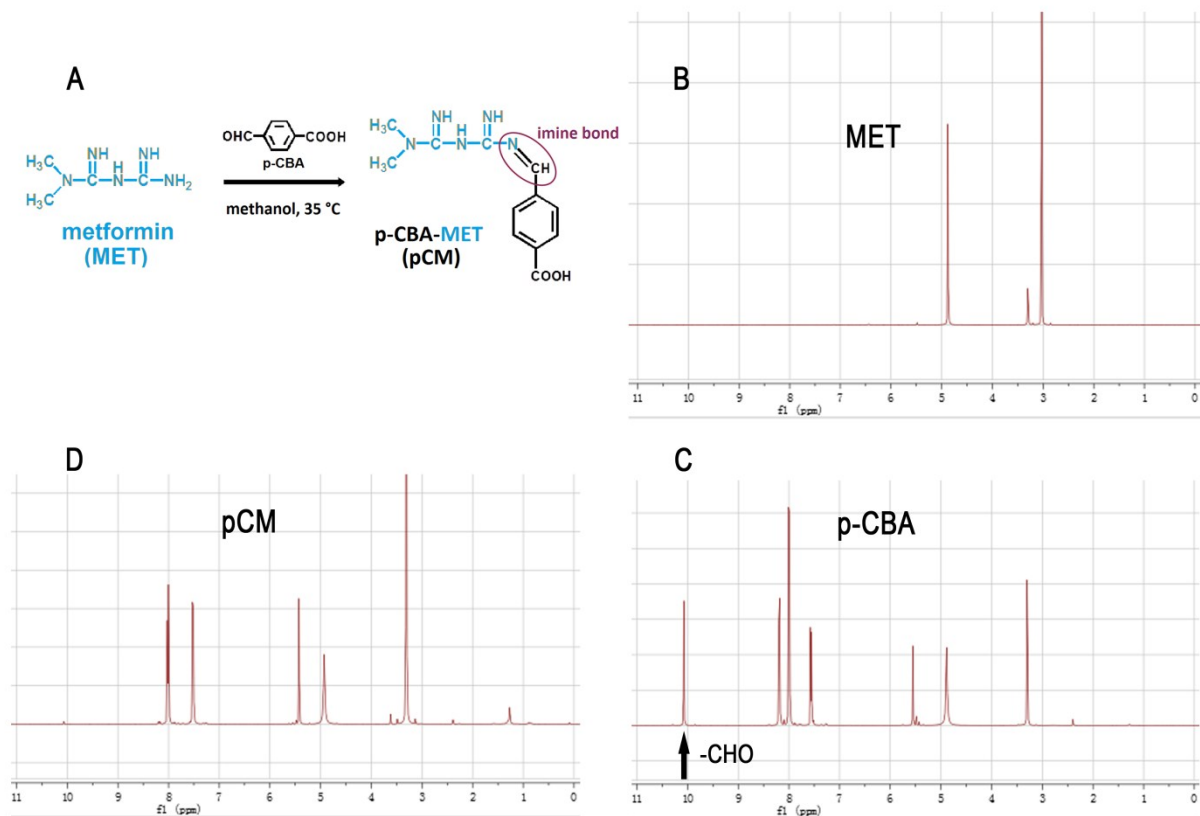
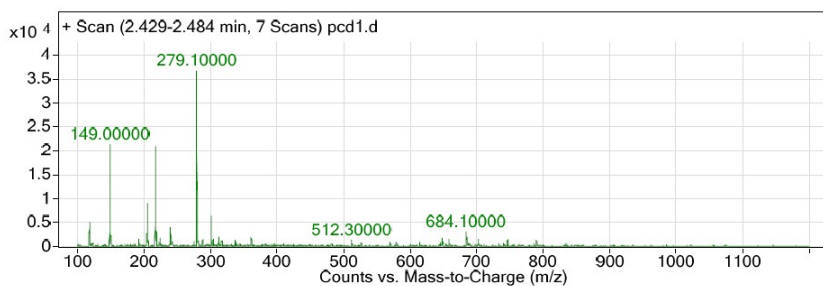


Figure S3. (A). Schematic illustration of p-CBA-MET (pCM). The $^1\text{H-NMR}$ spectrum of (B) MET, (C) p-CBA and (D) pCM (in CD_3OD). The arrow in (C) indicated the characteristic peak of aldehyde group in p-CBA. This peak disappeared in (D), indicating the formation of imine bonds.



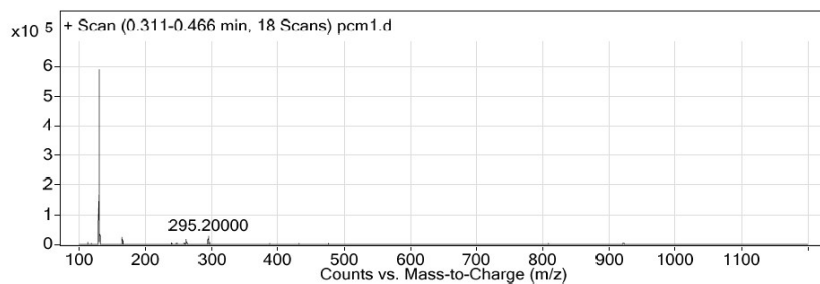
Peak List

<i>m/z</i>	<i>z</i>	Abund
118.1	1	5021.13
149	1	21333.21
205.1	1	8911.61
217.1	1	20938.71
218	1	3413.23
240		3967.54
279.1	1	36750.07
280.1	1	7597.2
301.2	1	6394.34
684.1	1	2983.64

Peak Identification

Peak (<i>m/z</i>)	Structure	Molecular formula	M.W.
149		C ₈ H ₆ O ₃	150
217		C ₁₃ H ₁₅ O ₂ N	217
279		C ₁₄ H ₁₇ O ₅ N	279

Figure S4. Mass spectrometry analysis result of pCD. Several characteristic peaks have been identified as shown in the figure.



Peak List		
<i>m/z</i>	<i>z</i>	Abund
113		5959.79
130.1	1	591297.69
131.1	1	38052.9
165.1		26446.95
262.1		18803.83
294.1		14275.12
295.2		28288.89
297.2		8597.02

Peak Identification

Peak (<i>m/z</i>)	Structure	Molecular formula	M.W.
130.1 / 131.1		C ₄ H ₁₁ N ₅	129
165.1		C ₄ H ₁₁ N ₅ ·HCl	165.5
262.1		C ₁₂ H ₁₅ O ₂ N ₅	261
294.1 / 295.2 / 297.2		C ₁₂ H ₁₅ O ₂ N ₅ ·HCl	297.5

Figure S5. Mass spectrometry analysis result of pCM. Several characteristic peaks have been identified as shown in the figure.

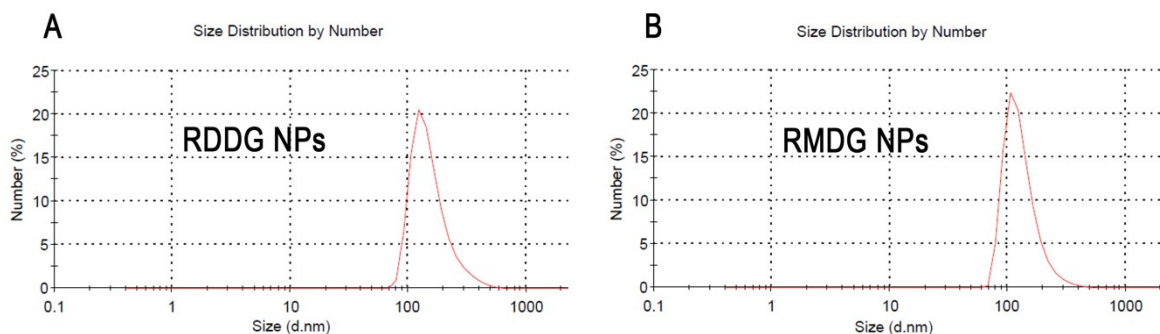


Figure S6. DLS size distribution of (A) RDDG NPs and (B) RMDG NPs. Measured in pH 8.0 PBS.

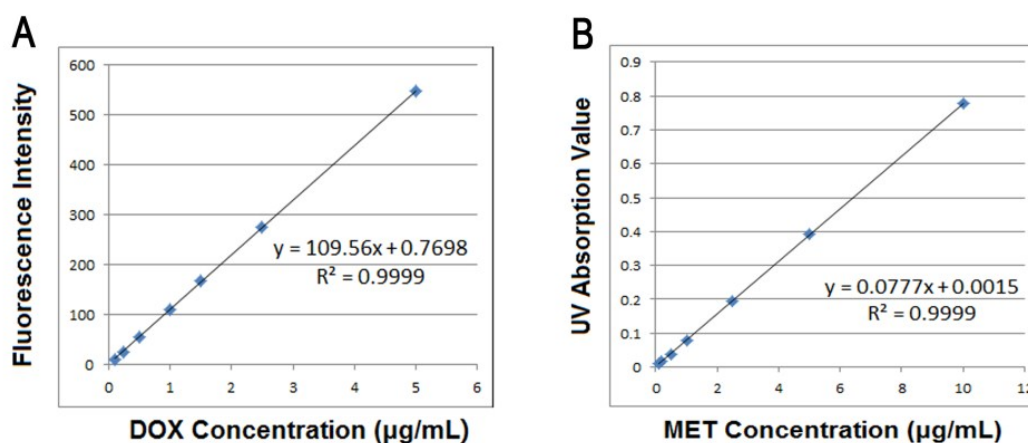


Figure S7. (A).Fluorescence standard curve of DOX ($E_x = 488 \text{ nm}$, $E_M = 555 \text{ nm}$) in DMSO. (B).UV absorption standard curve of MET ($\lambda = 233 \text{ nm}$) in deionized water.

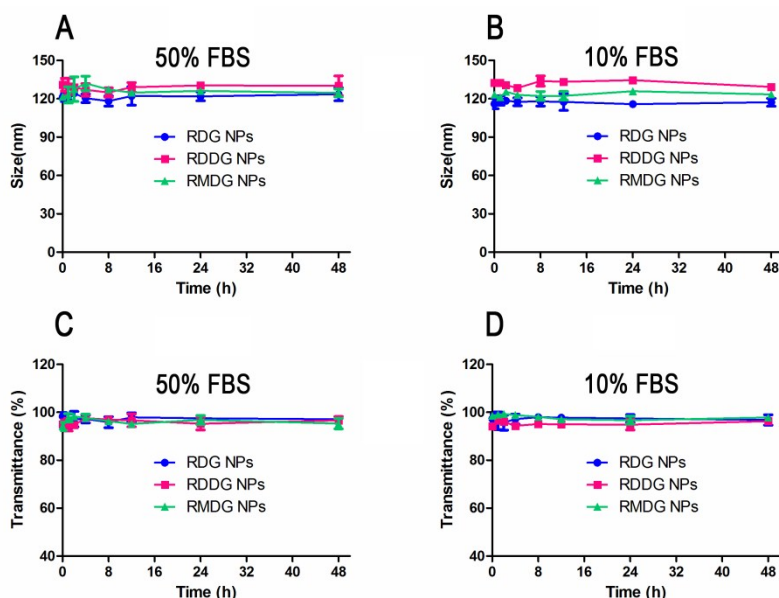


Figure S8. The serum stability of NPs. Particle size variation of NPs within a 48 h, 37 °C incubation with (A) 50% FBS or (B) 10% FBS. Transmittance variation of NPs within a 48 h, 37 °C incubation with (C) 50% FBS or (D) 10% FBS (means \pm SD, n = 3).

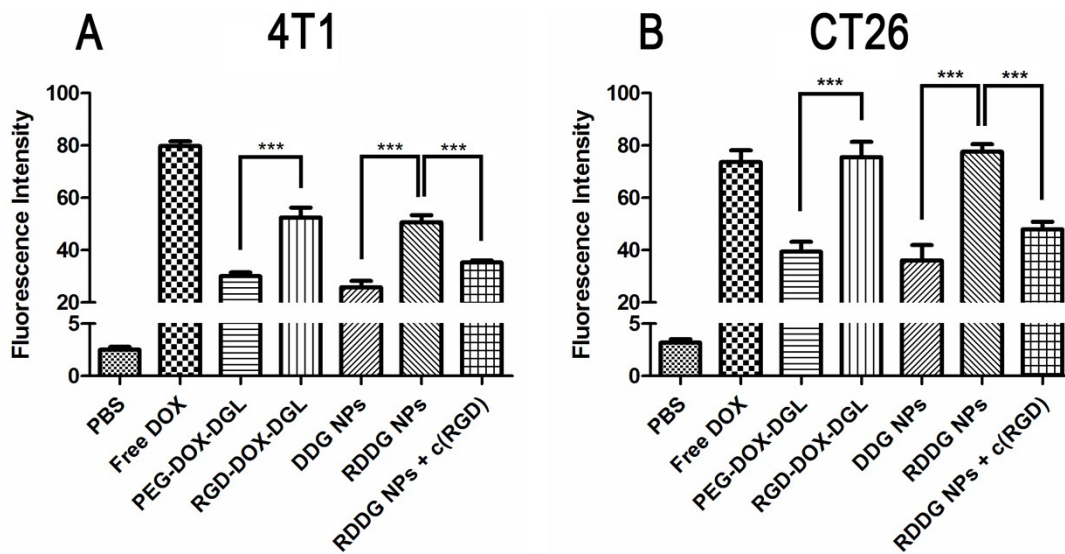


Figure S9. Quantitative cellular uptake results of (A) 4T1 and (B) CT26 cells. Cells were incubated with Free DOX, PEG-DOX-DGL, RGD-DOX-DGL, DDG NPs, RDDG NPs and RDDG NPs (cells pre-incubated with c(RGD) 0.5 h in advance) for 2 h. The equivalent dose of DOX was $5 \mu\text{g mL}^{-1}$. (means \pm SD, $n = 3$, *** $p < 0.001$)

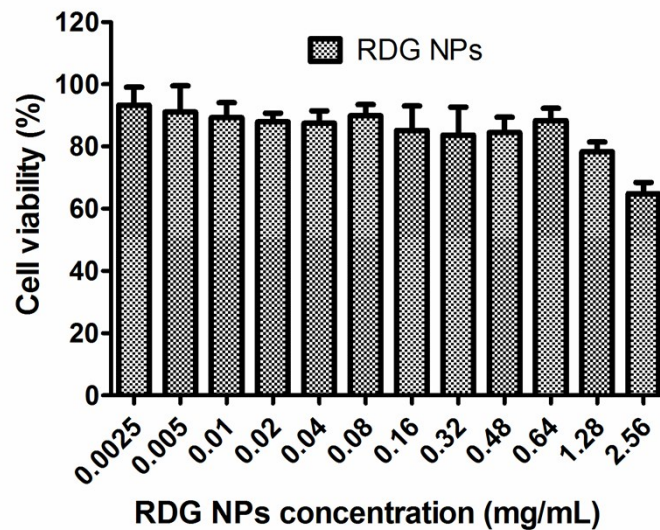


Figure S10. Cytotoxicity assay results of RDG NPs in 4T1 cells (means \pm SD, $n = 5$).

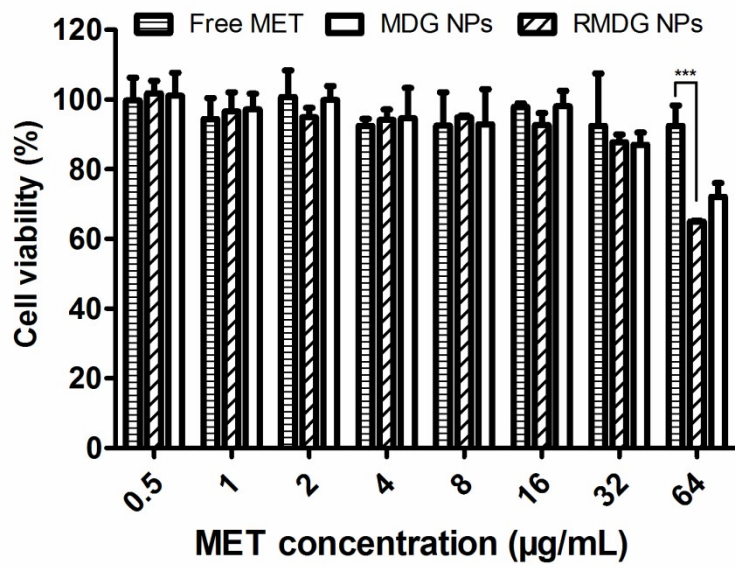


Figure S11. Cytotoxicity assay results of free MET, MET-DGL-GNP NPs (MDG NPs) and RMDG NPs in 4T1 cells (means \pm SD, $n = 5$, * $p < 0.05$, *** $p < 0.001$).

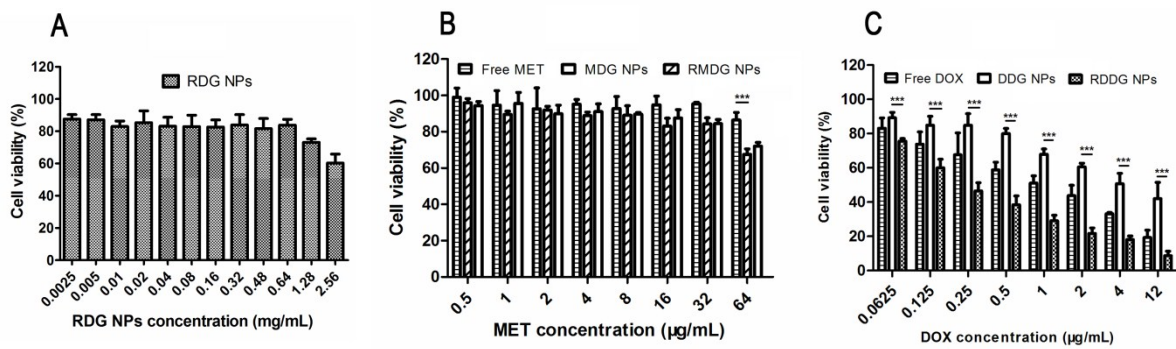


Figure S12. Cytotoxicity assay results of (A) RDG NPs, (B) MET preparations and (C) DOX preparations in CT26 cells (means \pm SD, $n = 5$, *** $p < 0.001$).

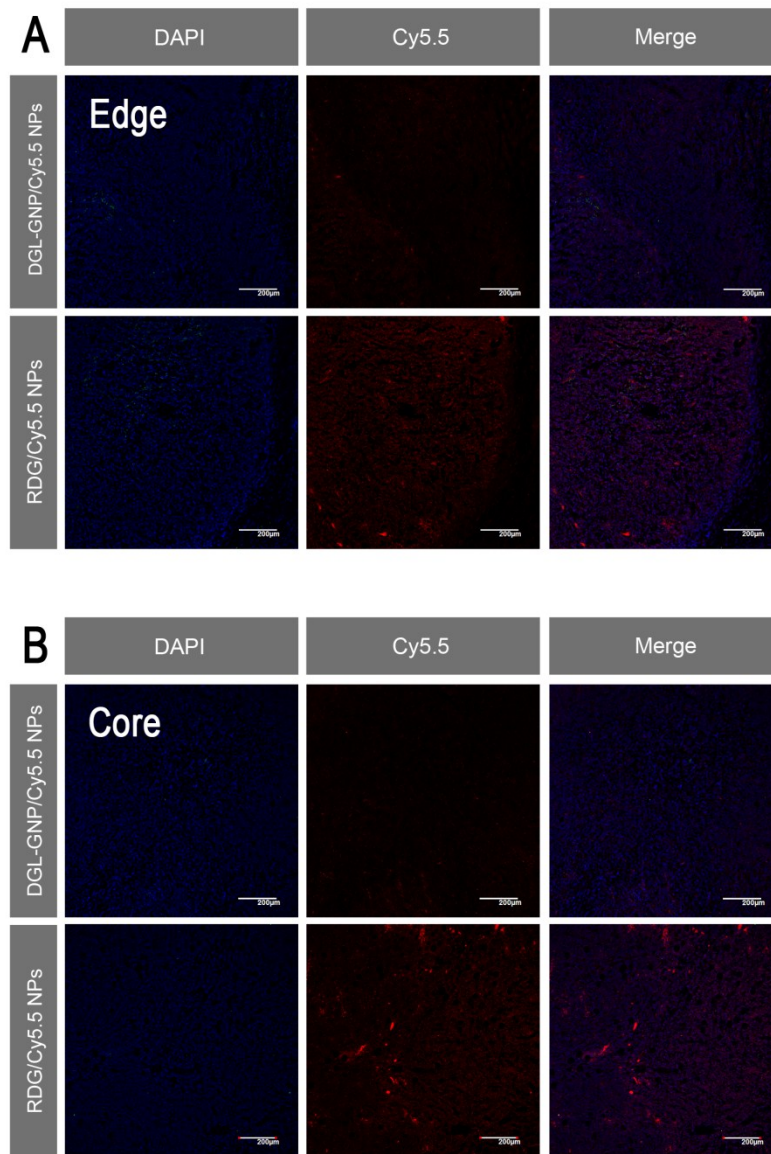


Figure S13. Frozen sections of 4T1 tumors at 24 h after the intravenous injection of Cy5.5-loaded NPs, showing blue (DAPI-stained nuclei) and red channel (Cy5.5) (scale bar = 200 μ m). Figure (A) shows the edge area of tumors and figure (B) shows the core area of tumors.

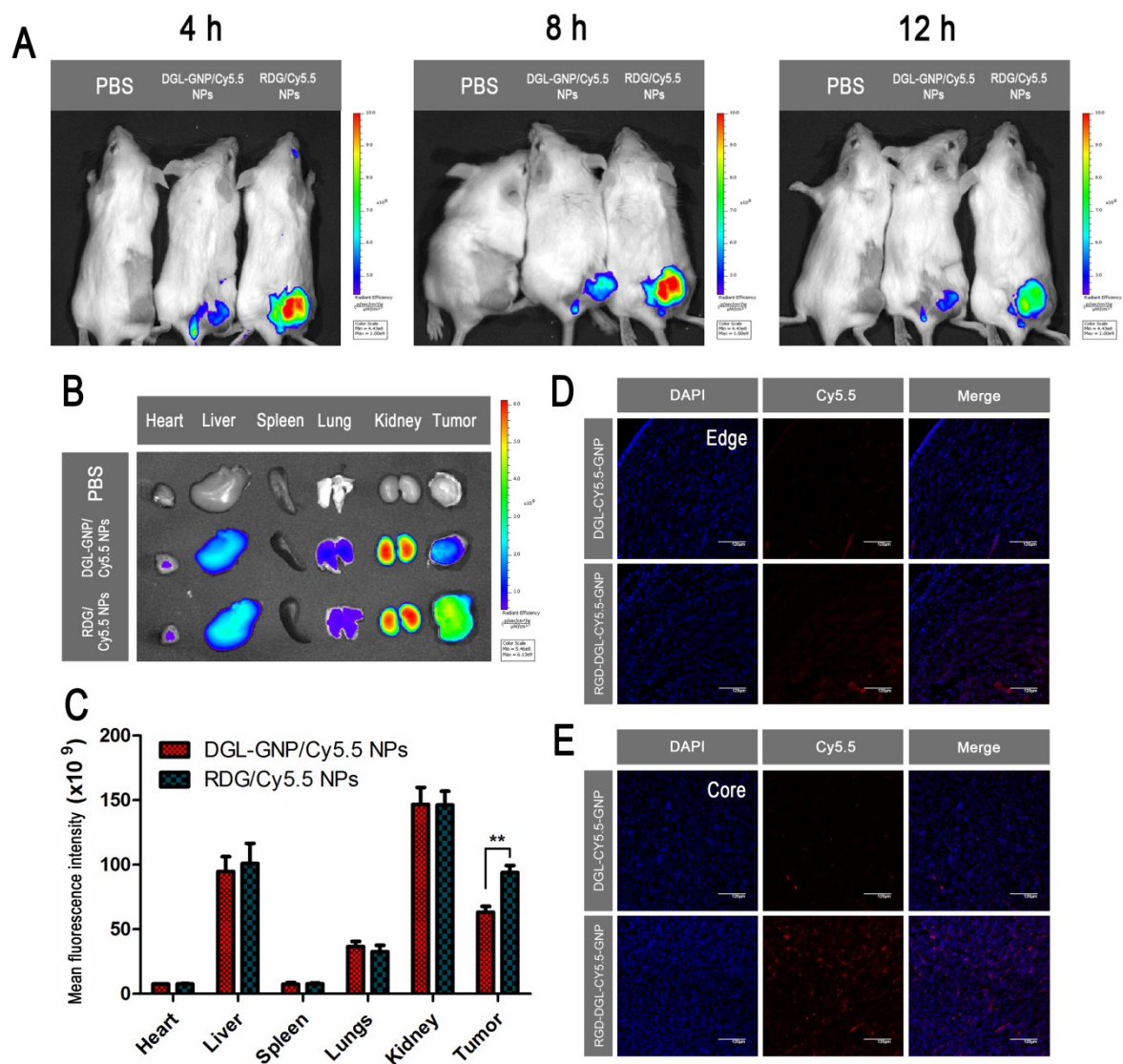


Figure S14. (A). Live images of CT26 tumor-bearing Balb/c mice at 4, 8 and 12 h and (B) *ex vivo* images of organs and tumors at 24 h after the intravenous injection of PBS, DGL-GNP/Cy5.5 NPs or RDG/Cy5.5 NPs (the equivalent dose of Cy5.5 was 30 μ g per mouse). (C). Semi-quantitative fluorescence intensity results of Cy5.5-loaded NP distribution in tumors and organs of CT26 tumor-bearing Balb/c mice at 24 h post intravenous injection (means \pm SD, n = 3). $** p < 0.01$ (D) and (E). Frozen sections of CT26 tumors at 24 h after intravenous injection of Cy5.5-loaded NPs, showing blue channel (DAPI-stained nucleus) and red channel (Cy5.5) (scale bar = 200 μ m). Figure (D) shows the edge area of tumors and figure (E) shows the core area of tumors.

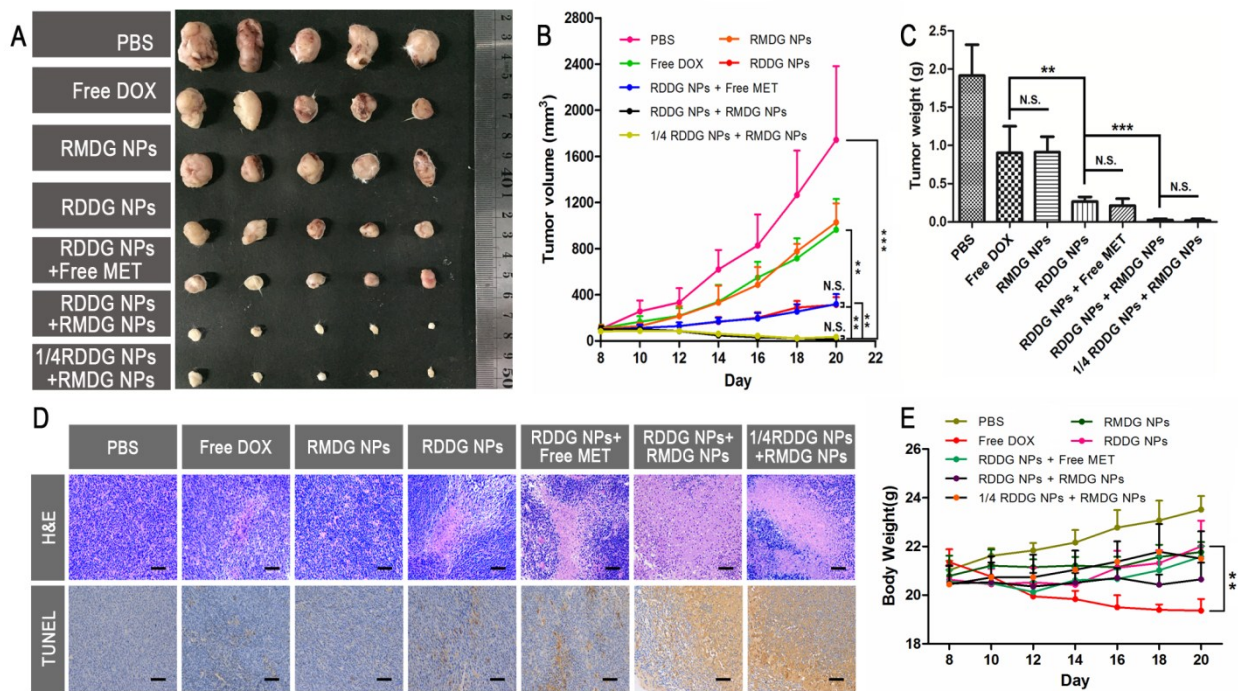


Figure S15. (A). Images of CT26 tumors harvested from tumor-bearing Balb/c mice on the 20th day of treatment. (B). Tumor growth curve of CT26 tumors after the systemic administration of different preparations. (means \pm SD, n = 6). ** $p < 0.01$, *** $p < 0.001$ (C). Weight of CT26 tumors in different groups (means \pm SD, n = 6). ** $p < 0.01$, *** $p < 0.001$ (D). Histological (H&E staining) and immunohistochemical analyses (TUNEL staining) of CT26 tumors. The necrotic region is stained pink by H&E. Apoptotic cells appeared brown following TUNEL staining (scale bar = 100 μ m). (E). Body weight curve of CT26 tumor-bearing mice (means \pm SD, n = 6). ** $p < 0.01$

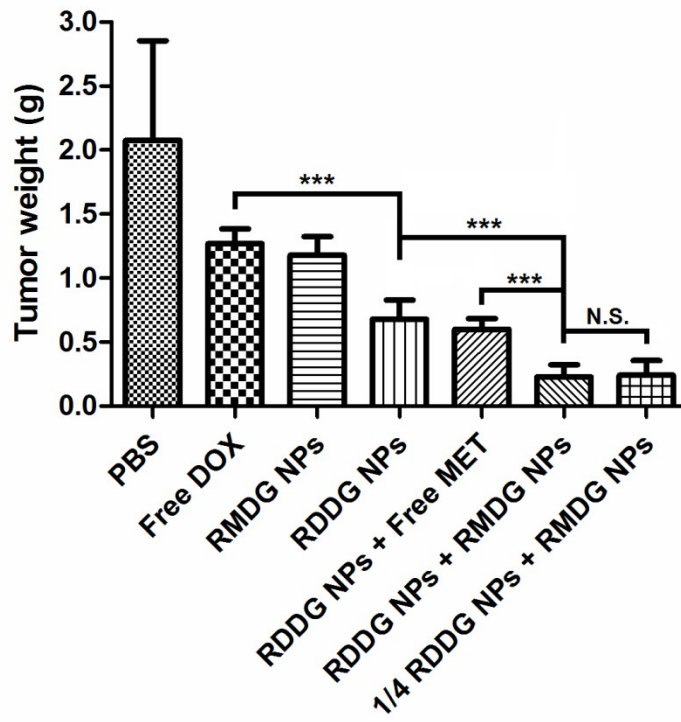


Figure S16. Weight of 4T1 tumors in different groups (means \pm SD, $n = 6$). ** $p < 0.01$, *** $p < 0.001$

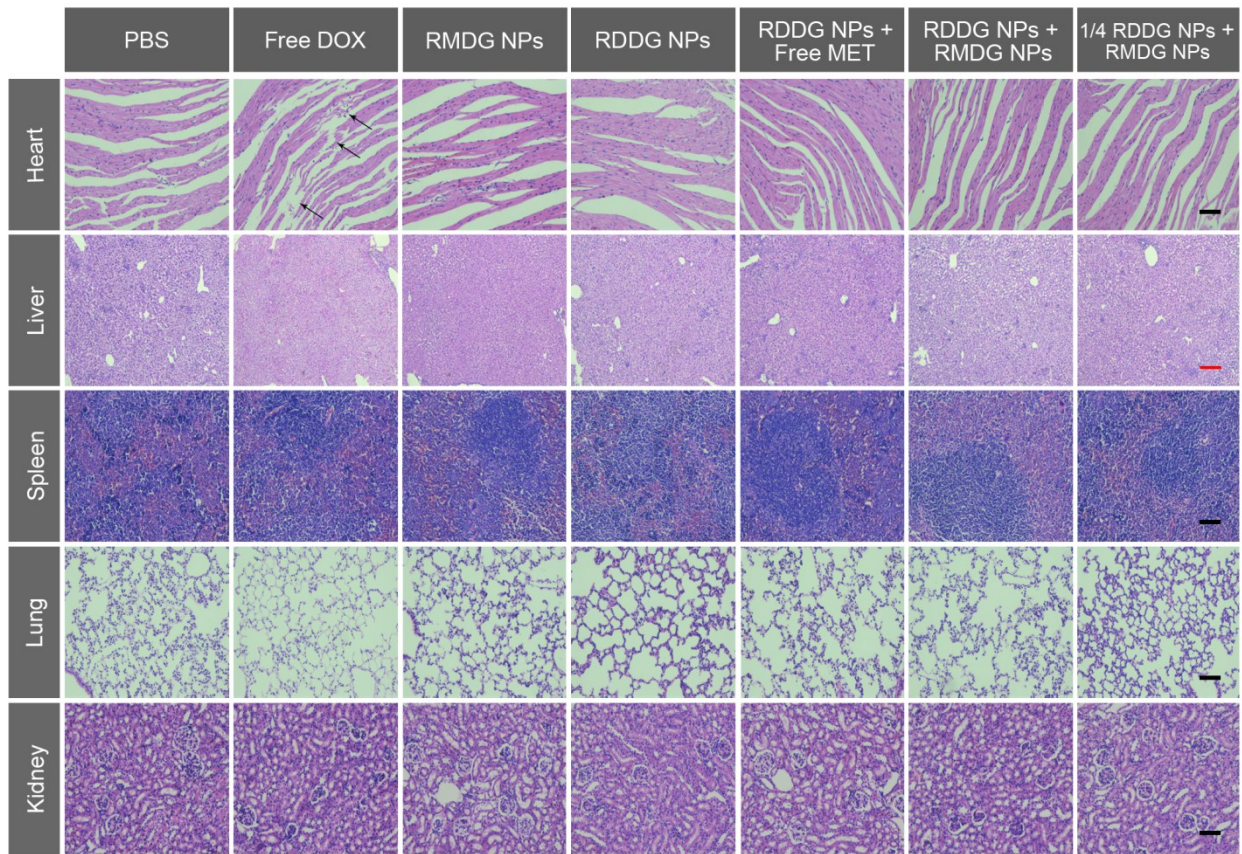


Figure S17. H&E staining analysis for major organs of 4T1 tumor-bearing mice on the 20th day of treatment. (Black scale bar = 100 μ m, red scale bar = 250 μ m). Arrows indicated the damaged cardiomyocytes.

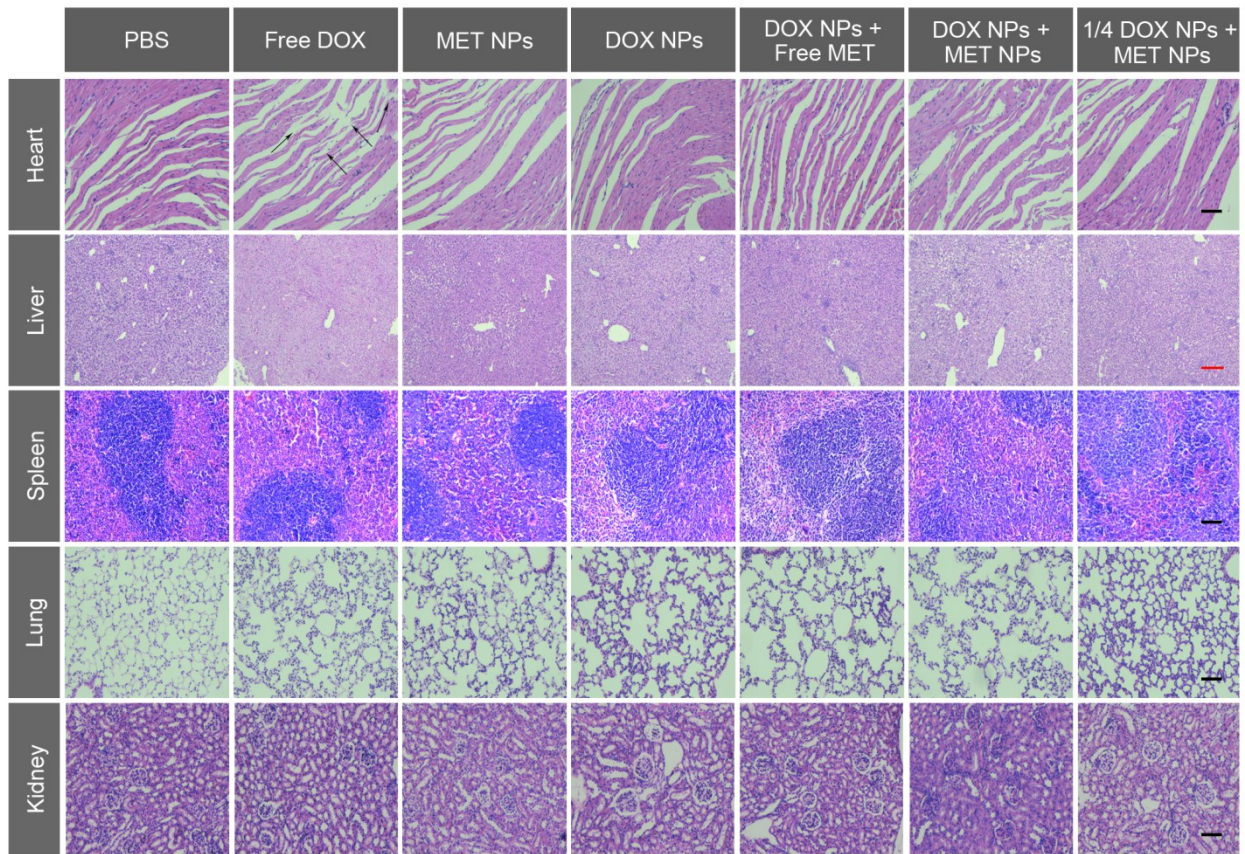


Figure S18. H&E staining analysis for major organs of CT26 tumor-bearing mice on the 20th day of treatment. (Black scale bar = 100 μ m, red scale bar = 250 μ m). Arrows indicated the damaged cardiomyocytes.

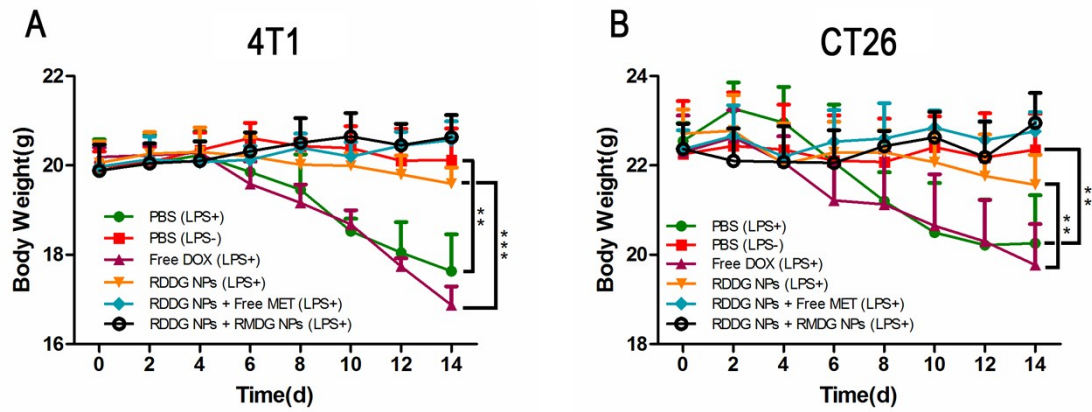


Figure S19. Body weight curve of (A) 4T1 metastasis model mice and (B) CT26 metastasis model mice (means \pm SD, n = 6). ** $p < 0.01$ and *** $p < 0.001$

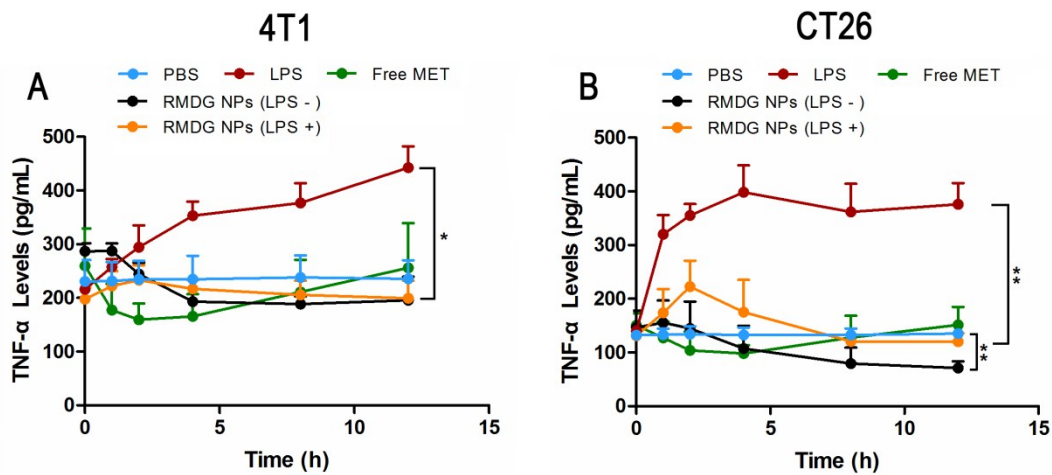
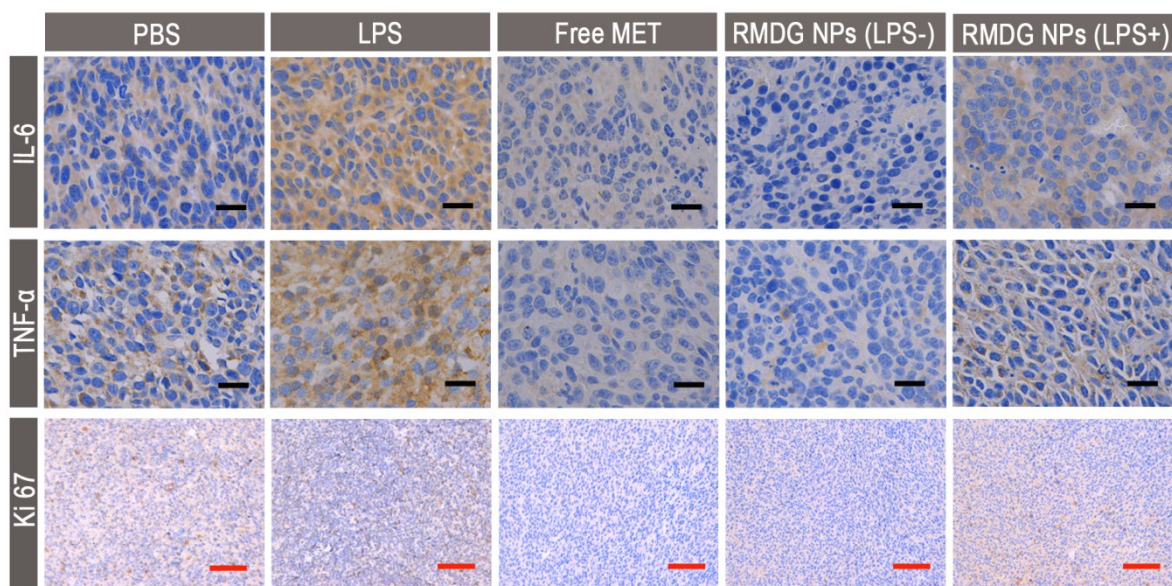


Figure S20. TNF- α expression level in (A) 4T1 mouse model and (B) CT26 mouse model after treatment with PBS (i.v.), free MET (i.v.), RMDG NPs (i.v.), RMDG NPs (i.v.) with LPS (i.p.) (at an equivalent dose of 5 mg kg⁻¹ MET) or PBS (i.v.) with LPS (i.p.) (0.5 μ g LPS in 0.1 mL PBS each) (means \pm SD, n = 3). * $p < 0.05$, ** $p < 0.01$



CT26

Figure S21. Immunohistochemical analysis (IL-6, TNF- α , Ki67) of CT26 tumors in different groups. IL-6, TNF- α and Ki67 were stained brown. (Black scale bar = 20 μ m, red scale bar = 100 μ m)

References for Supporting Information

1 C. Wong, T. Stylianopoulos, J. Cui, J. Martin, V. P. Chauhan, W. Jiang, Z. Popovic, R. K. Jain, M. G. Bawendi and D. Fukumura, *Proc. Natl. Acad. Sci. U. S. A.*, 2011, 108, 2426-2431.